Silicon (2024) 16:3473–3483
https://doi.org/10.1007/s12633-024-02931-y

RESEARCH

Modification and Development of the Structural, Morphological and Dielectric Characteristics of Polyvinyl Alcohol Incorporated with Cerium Dioxide / Silicon Carbide Nanoparticles for Nanodielectric and Nanoelectronic Applications

Ali Hussein Abdel-Amir[1] · **Majeed Ali Habeeb**[1]

Received: 16 December 2023 / Accepted: 25 February 2024 / Published online: 8 March 2024

Abstract
The objective of this study is to improve the electrical properties of nanostructures made of polyvinyl alcohol (PVA), silicon carbide (SiC), and cerium dioxide (CeO_2) so that they may be used in electronic nanodevices and flexible pressure sensors. Using a casting procedure, PVA/CeO_2/SiC films containing 0, 2, 4, 6, and 8 wt% CeO_2/SiC nanoparticles were produced. When the weight% of (PVA/CeO_2/SiC) nancomposites (NCs) films reaches 8%, field emission scan electron microscope (FE-SEM) investigation reveals cohesive aggregates or fragments that are randomly spread on the top surface. Unlike the pure (PVA) film, optical microscopy (OM) has shown that the (CeO_2/SiC) nanoparticles (NPs) form a network inside the polymer matrix. The FTIR study showed that the physical interaction between polymer matrix (PVA) and CeO_2/SiC nanoparticles. Analyses of the dielectric properties of PVA/CeO_2/SiC nanocomposites showed that, as frequency increased, both the dielectric constant and the dielectric loss decreased, while its increase when the ratio of (CeO_2/SiC)NPs increases. When the frequency and ratio of (CeO_2/SiC) NPs in (PVA/CeO_2/SiC) nanocomposites increase, the A.C electrical conductivity also increases. Results showed that the dielectric characteristics of PVA/CeO_2/SiC films improved with increasing pressure, suggesting that these nanostructures might be promising as pressure sensors. The outcomes of the pressure sensor's application show that the (PVA/CeO_2/SiC) nanostructures outperform competing sensors in terms of pressure sensitivity, flexibility, and environmental durability.

Keywords Structural properties · AC electrical properties · Nanocomposites · Pressure sensor

1 Introduction

The conjugated chains found in polymers give these organic compounds remarkable electrical conductivity. Their ability to transport charges via the π-electrons enables the mobility of charges along the polymer chains, which is the reason for this. There are a few benefits and drawbacks to using polymers, but overall, they are quite like inorganic compounds. Among them are its inexpensive cost, lightweight nature, simplicity of processing, resistance to corrosion, and high flexibility. Important features, such as resistance to heat and good mechanical qualities, are also present in the inorganic materials. Hence, the combination of polymers and inorganic compounds finds wide use in several fields [1]. Nanotechnology has the potential to enhance our quality of life in several ways, including the acceleration of electronic devices, the expansion of memory capacity, the reduction of energy costs by improving energy conversion efficiency, and the enhancement of security via the advancement of nanoscale technology [2]. Nanotechnology is a highly sought-after field for research and development across several technological fields. Nanotechnology has the potential to facilitate the creation of innovative materials that may be used to design and produce new properties and structures. This will lead to greater performance, lower maintenance costs, and increased usefulness [3]. Due to their many advantages, such as low manufacturing costs, high resilience

✉ Majeed Ali Habeeb
pure.majeed.ali@uobabylon.edu.iq

Ali Hussein Abdel-Amir
ali.mahdi.pure488@student.uobabylon.edu.iq

[1] College of Education for Pure Sciences, Department of Physics, University of Babylon, Babylon, Iraq

to fatigue, and exceptional corrosion resistance, polymer matrix nanocomposites have become indispensable to contemporary materials. Several physical properties, including electrical, structural, thermal, and optical, are significantly altered when nanoparticles are introduced into a polymer matrix [4, 5]. The significant attention given to metal-oxide nanoparticles is due to their remarkable chemical and physical properties, which differ from those of bulk materials. These nanoparticles find extensive use in many applications, such as solar cells, optoelectronics, sensing, and catalysis [6, 7]. One kind of thermoplastic polymer that exhibits partly crystalline properties is polyvinyl alcohol, or PVA. Notable properties include high water resistance, good interactions with biological things, non-toxicity, and long-term tolerance to chemical and mechanical stress. Among the many fields that make use of polyvinyl alcohol (PVA) are those dealing with implants, eye care, textiles, membranes, medicines, and personal care products [8]. Researchers are looking at polyvinyl alcohol (PVA) as a possible material for prosthetic articular cartilage. Polyvinyl alcohol (PVA) has considerable promise as a substance owing to its remarkable storage capability, elevated dielectric resistance, and distinctive electrical characteristics. This flexible material has several major uses, including polymer recycling, packaging, and drug delivery systems [9]. Of all the rare-earth metal oxide compounds, CeO_2 is one of the most attractive. Optical and photoelectric properties, thermal coatings, electrochemical cells, electromagnetic shielding, and corrosion protection are just a few of its many applications. Even though most rare-earth elements are only found in three-valent states, cerium may really exist in four-valent and trivalent forms. Its ability to alter oxidation states makes it useful in a variety of applications, such as solid oxide fuel cells and catalytic converters. In addition, CeO_2 is highly sought after for its unique qualities, which include being non-toxic, biocompatible, having the ability to store oxygen, and having remarkable optical and thermal characteristics. Its many useful properties make it an ideal material for use in biosensors, gas detectors, and solar cells, among other things [10, 11]. Chemically speaking, silicon carbide (SiC) is an example of a non-oxide substance. Ceramics used in semiconductors have several desirable properties, including high heat conductivity, resistance to oxidation, inertness to acids and melts, and thermal stability. Its great toughness and extraordinary stress resistance make it a popular choice for use in power-energy storage materials and microwave dielectrics. Consequently, it is possible to achieve outstanding outcomes. Surface-modified SiC nanoparticles enhance the performance of composites [12, 13]. The biomedical, aerospace, environmental, and automotive industries are just a few that rely on pressure sensors to control and monitor a wide range of applications. The pressure sensors made of nanocomposite materials may act in two ways: piezo resistively or pseudo-capacitive, depending on the circumstances. Differentiating pressure sensors is possible according to KPIs such as pressure range, sensitivity to small forces, resistance to larger forces, and pressure sensitivity [14, 15]. One possible method for measuring strain is the use of piezo resistive pressure sensors, which work by changing the resistance of test patterns in response to applied pressure. For the most part, piezo resistive pressure sensors are made from materials like polysilicon thin films, bonded metal foils, inkjet printer films, sputtered thin films, and silicon. Because of their low price and high sensitivity, The pressure sensor industry favors piezo resistive pressure sensors [16, 17]. This study introduces a straightforward and economical approach to fabricating nanocomposites of PVA, CeO2, and SiC suitable for nanoelectronics applications and flexible pressure sensors.

2 Experimental Part

Polyvinyl alcohol (PVA), cerium dioxide (CeO_2), and silicon carbide (SiC) nanocomposites were produced using the casting process. 1 g of PVA was dissolved in forty milliliters of distilled water and stirred with a magnetic stirrer for thirty minutes at seventy degrees Celsius to get a homogeneous solution. Subsequently, CeO_2 and SiC nanoparticles were introduced to the PVA solution at varying concentrations (0, 2, 4, 6, and 8 work percent). After the solution had dried at room temperature for five days, polymer nanocomposites were formed. We used the petri dish-clipped (PVA/CeO_2/SiC) NCs for our analysis. A Hitachi SU6600 variable pressure scanning electron microscope (FE-SEM) was used for the analysis of the structural characteristics of PVA/CeO_2/SiC NCs. An optical microscope (OM) supplied by Olympus (model Nikon-73346) was used to study the nanocomposites topically. A German-made Bruker vertex-70 Fourier transform infrared spectroscopy (FTIR) device having a 500–4000 cm–1 wavenumber range. The dielectric characteristics were examined using an LCR meter, the Hioki 3532–50 LCR HI TESTER, throughout the frequency range of 100 Hz to 5106 Hz. The pressure sensor of the PVA/CeO_2/SiC nanocomposites was tested by measuring the parallel capacitance between the specimen's top and bottom poles at different pressures (80–160 bar) using an LCR meter.

The following formula is used to compute the dielectric constant (ε′) [18, 19]:

$$\acute{\varepsilon} = \frac{C_p}{C_o} \tag{1}$$

The sign "(C_o)" is usually used to denote a vacuum capacitor, whereas the term "C_p" is generally used to describe

capacitance. It is possible to express the dielectric loss (ε") as [20, 21]:

$$\varepsilon'' = \acute{\varepsilon} D \tag{2}$$

The variable "displacement" (D) is utilized in this context. The calculation for the alternating current (A.C.) electrical conductivity is as follows [22, 23]:

$$\sigma_{AC} = \omega \acute{\varepsilon}\ \varepsilon_o \tag{3}$$

where ω represents the angular frequency.

3 Results and Discussion

3.1 Field Emission Scanning Electron Microscope (FE-SEM) Measurements of (PVA/ CeO_2/SiC) Nanocomposites

Finite element scanning electron microscopy (FE-SEM) examination, which looks at how the nanoparticles are distributed within the polymer, confirms that the CeO_2/SiC particles have an effect on the NCs. Nanocomposites of PVA, CeO_2, and SiC with varying concentrations of CeO_2 and SiC NPs are shown in Fig. 1 by means of FE-SEM pictures. As the concentration of (CeO_2/SiC) NPs increases, the surface profile of the scheme changes, leading to the development of (PVA/CeO_2/SiC) nanocomposites. Image (a) clearly shows

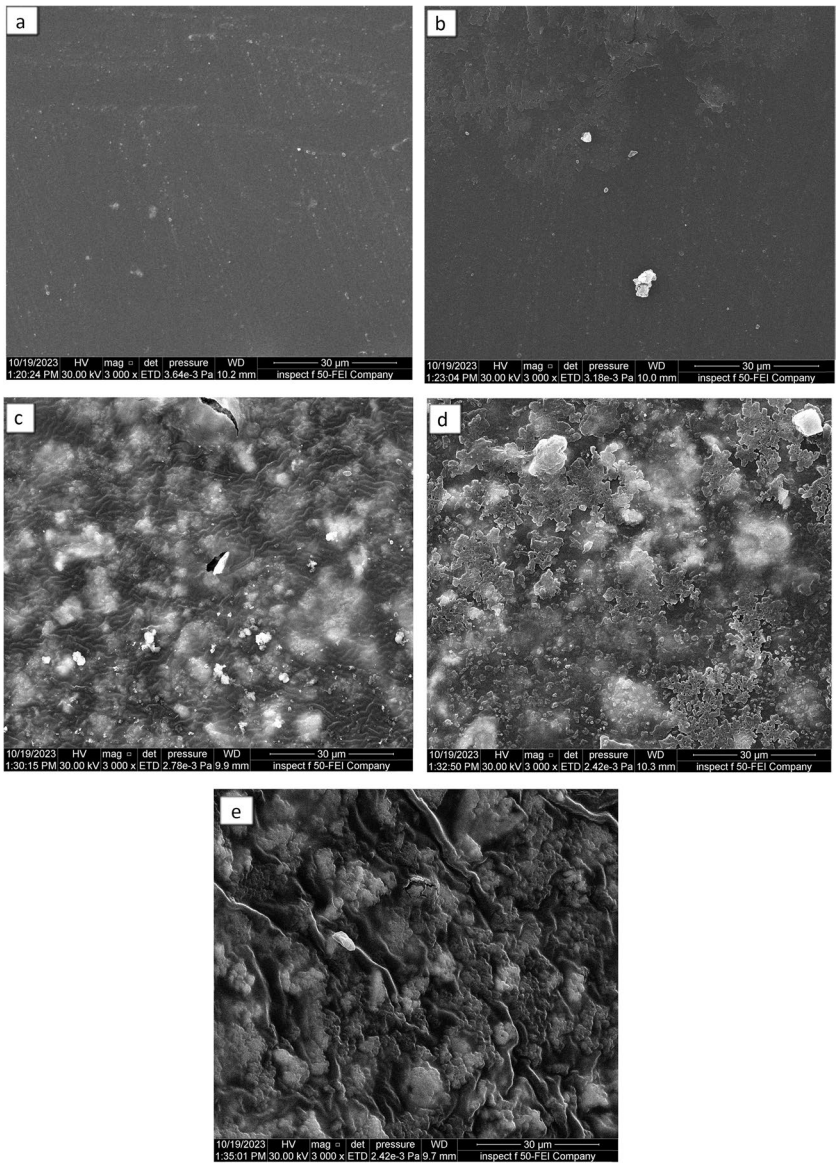

Fig. 1 FE-SEM images for (PVA/CeO_2/SiC) NCs: **a** PVA, **b** 2 wt% CeO_2/SiC, **c** 4 wt% CeO_2/SiC, **d** 6 wt% CeO_2/SiC, **e** 8 wt% CeO_2/SiC

the cohesive and homogeneous character of the polymer. Image (b), image (c), image (d), and image (e) all reflect this. As can be seen in the images shown, the presence of grain collections is proportional to the rise in CeO_2/SiC NP concentration. The PVA/CeO_2/SiC membranes' surface morphology will be determined by the findings. A higher concentration of (CeO_2/SiC) NPs causes a more even distribution of clusters or fragments over the nanocomposites' top surface [24–26].

3.2 The Optical Microscope of (PVA/CeO_2/SiC) NCs

Figure 2 exhibits optical microscope images of nanocomposite films composed of PVA/CeO_2/SiC at various concentrations, with a magnification of 10x. Nevertheless, the photographs clearly show significant disparities among them (a, b, c, d, and e). When the concentration of CeO_2/SiC NPs in (PVA) films reaches 8% weight percent, the CeO_2/SiC NPs create interconnected networks inside the polymer. The network's channels allow charge carriers to move freely within nanocomposites [27–29].

3.3 The FTIR Spectra of (PVA/CeO_2/SiC) Nanocomposites

Figure 3 displays the Fourier transform infrared spectra (500–4000 cm^{-1}) of (PVA/CeO_2/SiC) nanocomposites. The OH stretching vibrations in the main chain and aromatic rings are equivalent to the absorption band of pure PVA at 3262.55 cm^{-1} in picture (A) [28]. Among the vibrations attributable to C-H bonds are those at 2916.56 cm^{-1}, 1415.42 cm^{-1}, and 1085.37 cm^{-1}, all of which correlate to the C-O bond in carbohydrates [30–32]. The inorganic carbonate bands at 837.84 cm^{-1} that correspond to the bending -C=O bond. Images B, C, D, and E show the spectra of PVA with varying concentrations of CeO_2 and SiC NPs added. In picture B, the inclusion of 2 wt% CeO_2 and SiC NPs shifted the wavenumber to a low value in certain bands and intensities at (32,386.63, 1412.60, 1084.36) cm^{-1}, whereas the bands 2920.27 cm^{-1} and 838.87 cm^{-1} shifted to a high value. In the picture C, the additive concentration of 4 wt.% from CeO_2 and SiC NPs resulted in a shift to lower wavenumbers for the bands at 2918.01 cm^{-1} and 1319.18 cm^{-1}. Conversely, the bands at 3245.35 cm^{-1}, 1084.76 cm^{-1}, and 839.50 cm^{-1} saw a shift to higher wavenumbers.

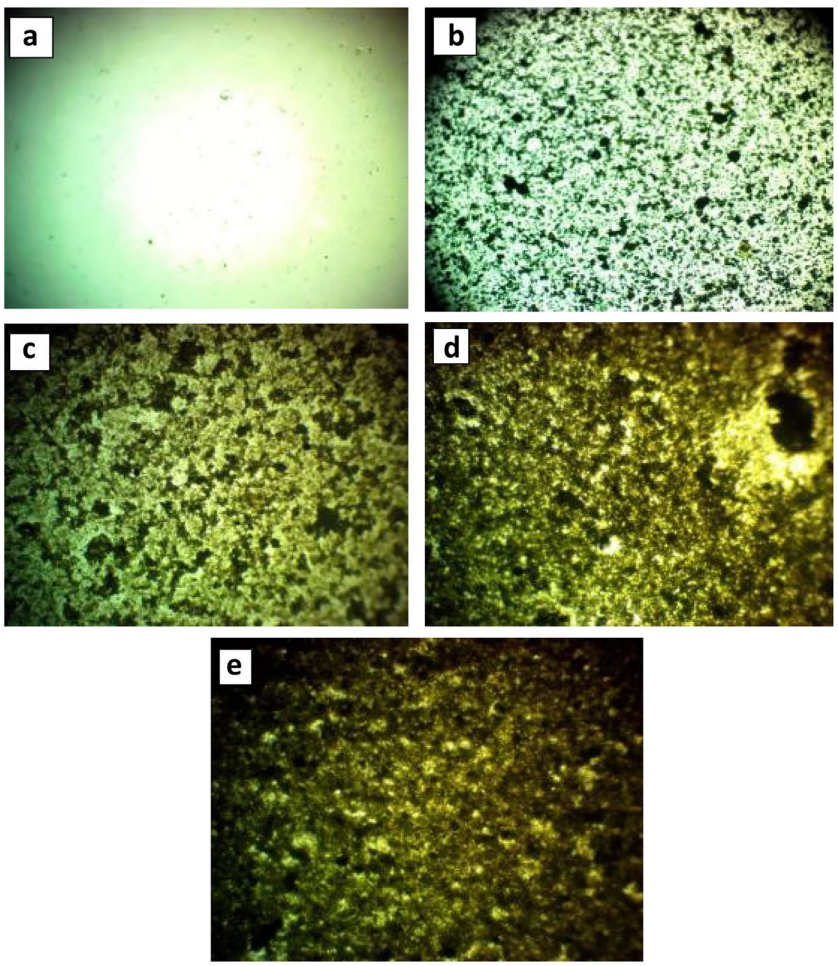

Fig. 2 Optical microscope images for (PVA/CeO_2/SiC) samples: **a** for PVA, **b** 2 wt% CeO_2/SiC NPs, **c** 4 wt% CeO_2/SiC NPs, **d** 6 wt% CeO_2/SiC NPs, **e** 8 wt% CeO_2/SiC NPs

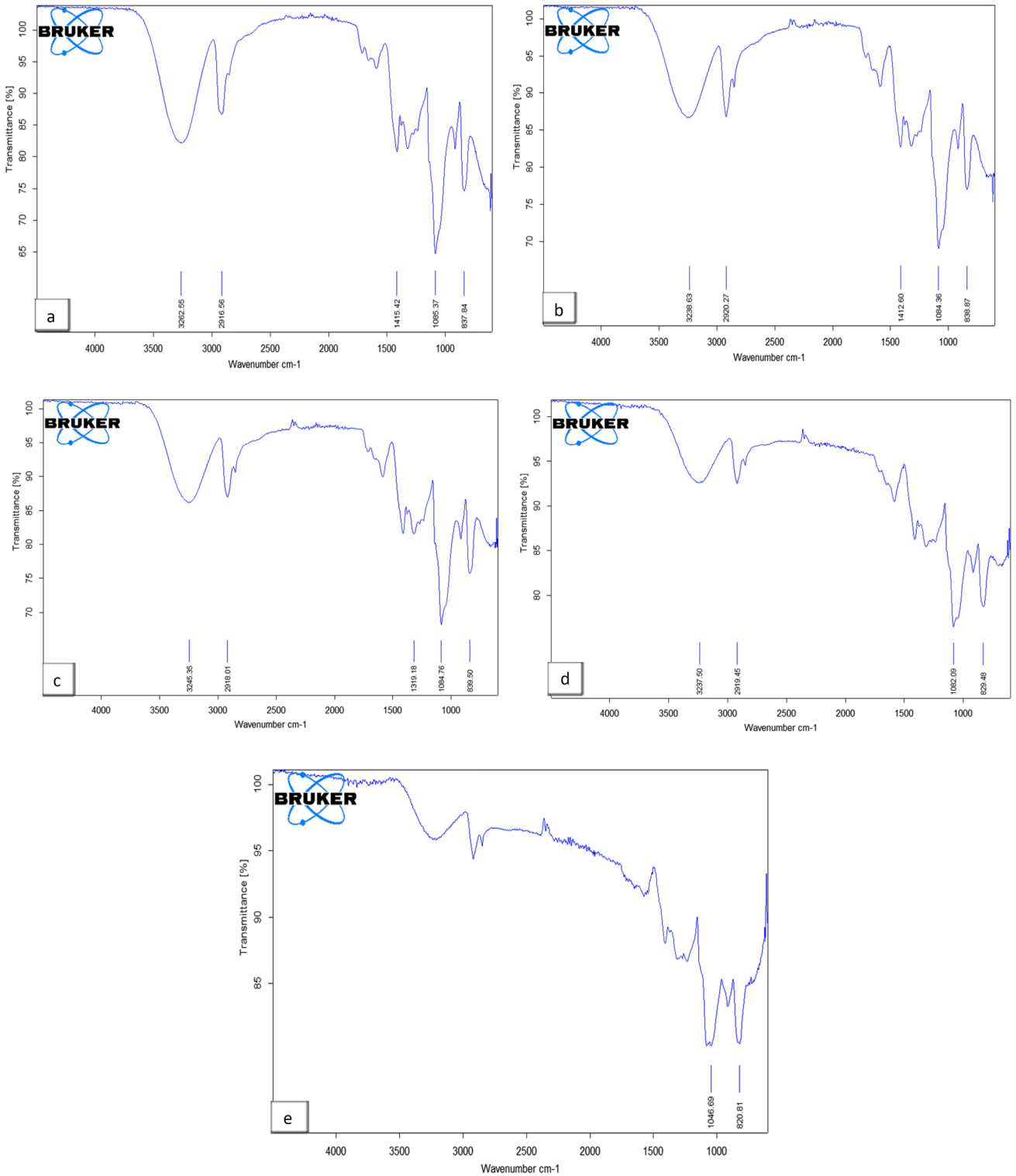

Fig. 3 FTIR data for PVA/CeO_2/SiC films: **a** for PVA, **b** 2 wt% CeO_2/SiC NPs, **c** 4 wt% CeO_2/SiC NPs, **d** 6 wt% CeO_2/SiC NPs, **e** 8 wt% CeO_2/SiC NPs

Image D shows that the bands at 3237.50, 1082.09, and 829.48 cm^{-1}, which are 6 wt% NPs, shifted to a low wave number; band 2919.45 cm^{-1}, on the other hand, shifted to a high wave number; and band 1319.18 cm^{-1}, in that region, was unaffected. The band (1046.69, 820.81) cm^{-1} in picture E changed to a low wave number due to the 8wt.% additive concentration

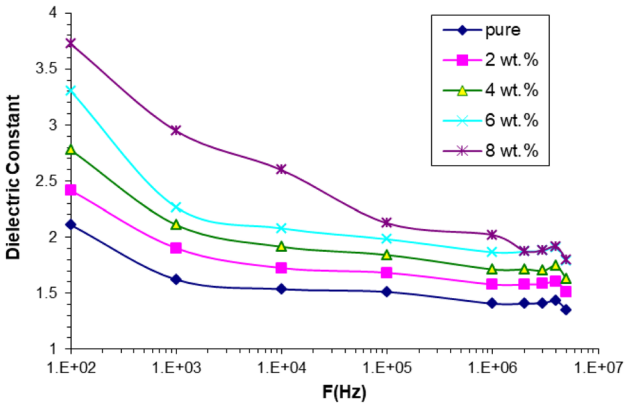

Fig. 4 Behavior of (έ) with a frequency for (PVA/CeO_2/SiC) nanocomposites

of NPs, whereas the band (3237.50, 2919.45, 1319.18) cm^{-1} remained unaffected. The FTIR analysis demonstrated that PVA, CeO_2, and SiC NPs do not interact chemically [33, 34].

3.4 The Dielectric Properties for PVA/CeO_2/SiC NCs

Equation (1) was used to determine the (PVA/CeO_2/SiC) NCs dielectric constant (έ). The correlation between frequency and dielectric constant is shown in Fig. 4. The ratio of space charge to total polarization decreases as the applied frequency increases, as indicated by the decreasing trend of the dielectric constant values. The most common kind of polarization in the low-frequency region is space charge polarization. The more often it occurs, though, the less important it becomes. Every PVA/CeO_2/SiC sample has a lower dielectric constant value as the electric field frequency increases because different kinds of polarization happen at higher frequencies. Because ions and electrons have different masses, ionic polarization reacts differently to changes in field frequency than electronic polarization [35–37].

Modifications to the dielectric constant of (PVA/CeO_2/SiC) NCs at 100 Hz as a function of CeO_2/SiC nanoparticle concentration are shown in Fig. 5. The dielectric constant of NCs is proportional to the concentration of CeO_2/SiC NPs. It

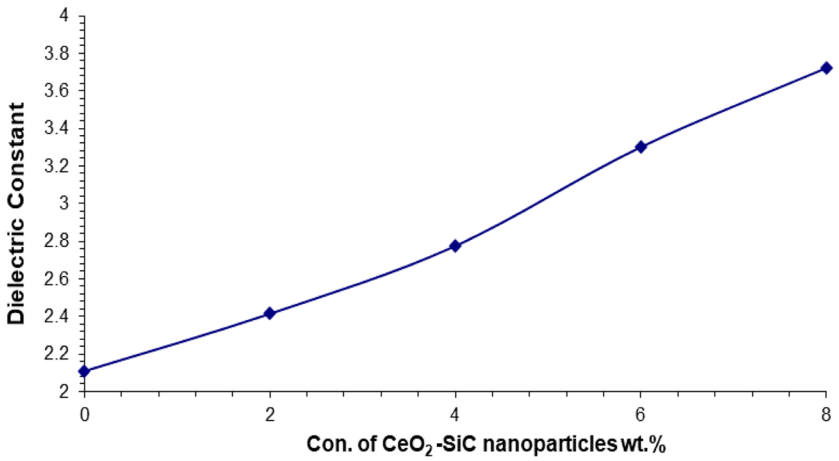

Fig. 5 Influence for (CeO_2/SiC) nanoparticles content on the (έ) for (PVA/CeO_2/SiC) nanocomposites at 100 Hz

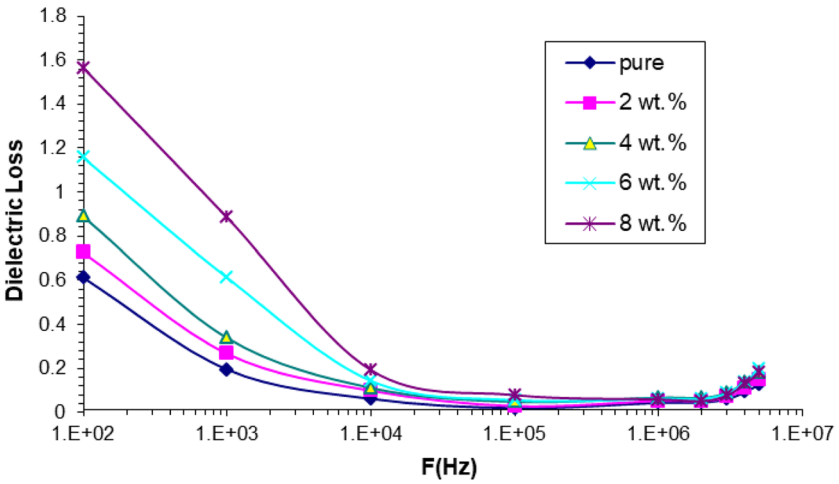

Fig. 6 Behavior of (ε˝) with a frequency for (PVA/CeO_2/SiC) nanocomposites

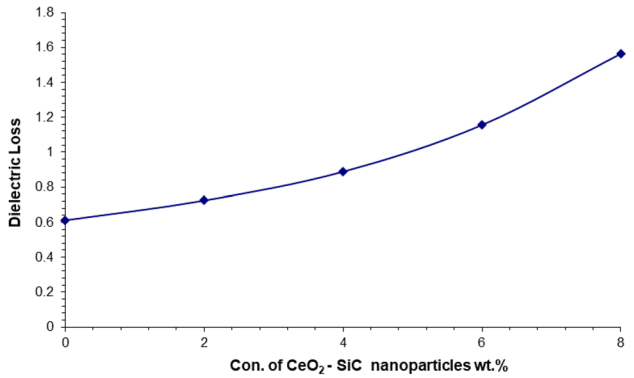

Fig. 7 Influence of (CeO_2/SiC) nanoparticles content on the (ε˝) for (PVA/CeO_2/SiC) nanocomposites at 100 Hz

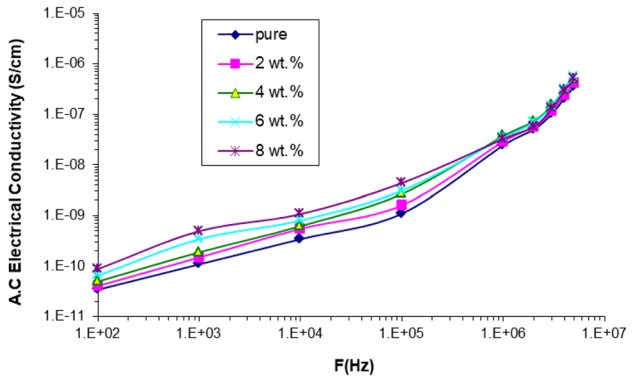

Fig. 8 Difference of electrical conductivity for (PVA/CeO_2/SiC) NCs with frequency

is possible that the extra charge carrier activity is due to interfacial polarization, which happens when an oscillating electric field divides two surfaces inside nanocomposites [38–40].

3.5 The Dielectric Loss for (PVA/CeO_2/SiC) NCs

Using Eq. (2), the dielectric loss (ε˝) of NCs was calculated. Dielectric loss characteristics of (PVA/CeO_2/SiC) NCs as a function of frequency are shown in Fig. 6. As seen in the picture, the dielectric loss is most apparent at lower applied frequencies and gradually reduces as the frequencies increase. The observed phenomenon is explained by the fact that the effect of space charge polarisation diminishes with increasing frequency [41–43].

The relationship between the dielectric loss (ε˝) and the concentration of CeO_2/SiC NPs is shown in Fig. 7. A significant association is seen between the concentration of nanoparticles and the dielectric loss of PVA/CeO_2/SiC nanocomposites, suggesting an increase in charge carriers [44, 45].

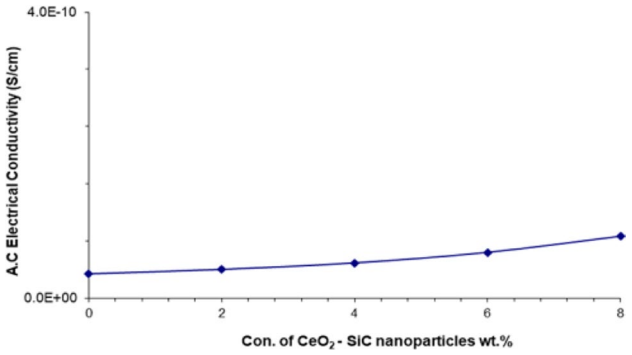

Fig. 9 Difference of electrical conductivity for (PVA/CeO_2/SiC) nanocomposites with (CeO_2/SiC) nanoparticles

Table 1 Results of the A.C. electrical conductivity, dielectric loss, and dielectric constant for NCs composed of (PVA/CeO_2/SiC) at 100 Hz

Con.(wt.) %	Dielectric constant	Dielectric loss	AC electrical conductivity(S/cm)
0	2.11	0.61	3.4E-11
2	2.41	0.72	4.03E-11
4	2.77	0.88	4.94E-11
6	3.3	1.15	6.43E-11
8	3.72	1.56	8.69E-11

3.6 The A.C Electrical Conductivity for (PVA/CeO_2/SiC) NCs

The alternating current electrical conductivity was determined by utilizing Eq. (3). Figure 8 depicts the correlation between frequency and electrical conductivity of (PVA/CeO_2/SiC) NCs. The graph presented depicts a significant rise in electrical conductivity with increasing frequency. This phenomenon is believed to be caused by space charge polarization occurring at low frequencies, as well as the hopping process that facilitates the movement of charge carriers [46, 47]. At higher frequencies, the observed increase in electrical conductivity is relatively minimal due to the phenomenon of electronic polarization and the movement of charge carriers through hopping [48, 49].

The impact of CeO_2/SiC nanoparticles on the (A.C) electrical conductivity of PVA/CeO_2/SiC nanocomposites at 100 Hz is shown in Fig. 9. Nanocomposites show a positive correlation between the electrical conductivity and the concentration of CeO_2 and SiC NPs. Dopant nanoparticles increase the number of charge carriers in nanocrystals (NCs), which lowers their resistance and improves their electrical conductivity [50, 51]. At a frequency of 100 Hz, Table 1 shows the values of the dielectric constant, dielectric loss, and A.C. electrical conductivity.

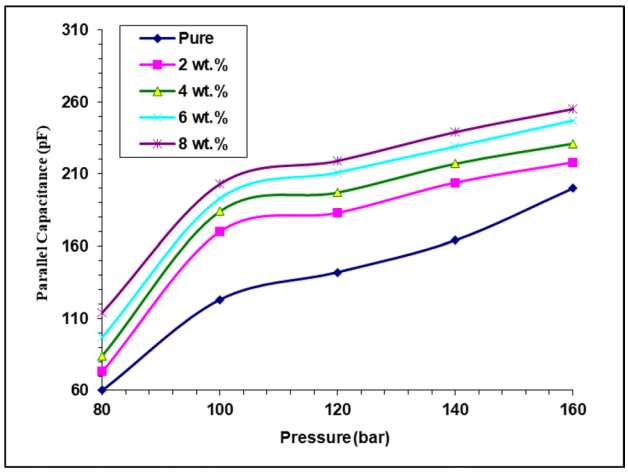

Fig. 10 Difference of parallel capacitance for (PVA/CeO_2/SiC) nanocomposites with pressure

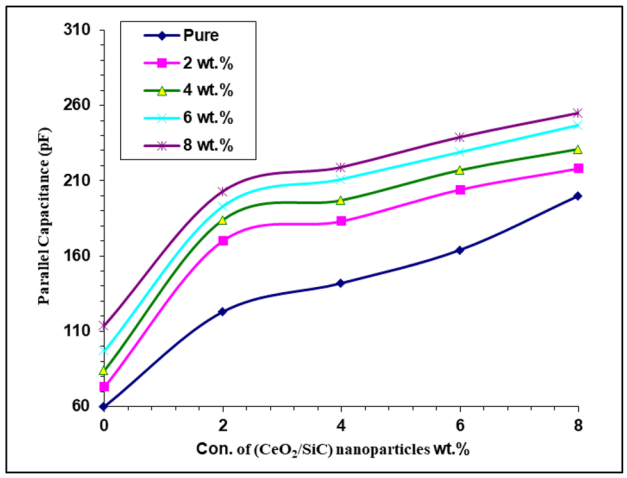

Fig. 11 Effect of (CeO_2/SiC) nanoparticles concentrations on parallel capacitance for (PVA/CeO_2/SiC) nanocomposites

3.7 Application of (PVA/CeO_2/SiC) NCs for Pressure Sensors

The parallel capacitance of (PVA/CeO_2/SiC) nanocomposites changes with pressure at different concentration of (CeO_2/SiC) nanoparticles, as shown in Fig. 10. An immediate correlation between the amount of the applied pressure and the capacitance is shown in the figure. The presence of crystalline areas with an internal dipole moment inside the nanocomposite samples explains the association between the applied pressure and the parallel capacitance. The dipole moments exhibit a stochastic orientation in the absence of any external mechanical or electrical effect, resulting in a dipole moment of zero amplitude [52, 53]. An electric field in the proximal distribution may be generated by subjecting the specimens to stress, which in turn can cause dipole moment changes. The creation of an electric field causes charges to accumulate at the sample's top and lower surfaces [54, 55].

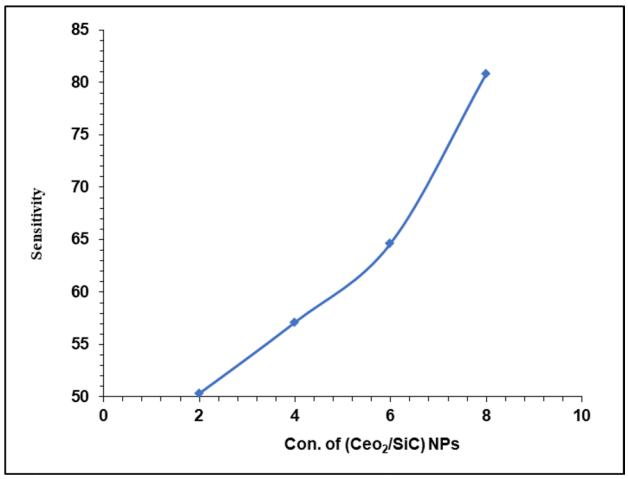

Fig. 12 Influence of (CeO_2/SiC) NPs concentrations on sensitivity for (PVA/CeO_2/SiC) nanocomposites

Table 2 Values of sensitivity with (CeO_2/SiC) NPs concentration for (PVA/CeO_2/SiC) nanocomposites

Con.(wt.) %	Sensitivity
2	50.3
4	57.1
6	64.7
8	80.9

In Fig. 11, we can see the relationship between the concentration of CeO_2/SiC nanoparticles at 80 bar and the electrical capacitance (C_p) of (PVA/CeO_2/SiC) nanocomposites. According to the graph, there is a positive correlation between the concentration of (CeO_2/SiC) nanoparticles and the electrical capacitance of nanocomposites. One possible explanation for the aforementioned phenomenon is the increased density of charge carriers inside nanocomposites [56, 57].

The effectiveness of (PVA/CeO_2/SiC) nanostructures is greatly affected by the concentration of (CeO_2/SiC) nanoparticles in the sensitive layer. The aforementioned phenomena dictates the range of pressure sensing, which in turn leads to a wide variety of uses requiring resistance to greater forces. In Fig. 12, we see how (CeO_2/SiC) nanoparticles affect the sensitivity of (PVA/CeO_2/SiC) nanocomposites. There is a positive correlation between the concentration of (CeO_2/SiC) NPs and the sensitivity of nanocomposites, as seen clearly in the graph, the occurrence may be explained by the internal dipole moment, as previously stated [58, 59]. Table 2 show values of sensitivity with concentration of (CeO_2/SiC) NPs for (PVA/CeO_2/SiC) NCs.

4 Conclusions

The current work involved preparation of (PVA/CeO_2/SiC) nanocomposites by using the solution casting technique. The structural, morphological and dielectric properties of (PVA/CeO_2/SiC) nanocomposites are examined. Field emission scanning electron microscope (FE-SEM) images show that the CeO_2/SiC nanoparticles were successfully dispersed within the PVA polymer matrix. The findings of optical microscope (OM) validated the hypothesis that the PVA, with its uniform surface and refined structure, demonstrated outstanding miscibility. The polymer nanocomposite films also showed evenly distributed additive concentrations of CeO_2/SiC NPs. The physical interaction between the polymer matrix and the CeO_2/SiC nanoparticles was confirmed by the Fourier transform infrared spectroscopy (FTIR) analysis. The dielectric characteristics of PVA/CeO_2/SiC nanostructures demonstrated that, at f = 100 Hz, the dielectric constant, dielectric loss, and A.C electrical conductivity all increase from (2.11 to 3.72), (0.61 to 1.56), and (3.4×10^{-11} to 8.69×10^{-11}) S/cm, respectively, as the concentration of CeO_2/SiC nanoparticles rose. Despite an increase in electrical conductivity (A.C), the dielectric constant and dielectric loss decrease with increasing frequency. Results showed that the dielectric characteristics of (PVA/CeO_2/SiC) nanostructures increased with increasing pressure, suggesting that these nanostructures might be useful as pressure sensors. An outstanding sensitivity of 80.9% is shown by the nanocomposites at a concentration of 8 wt %. Results of structural morphological, and dielectric properties confirmed that the PVA/CeO_2/SiC nanostructures might benefit in numerous pressure sensors and nanoelectronics applications.

Acknowledgements Acknowledgements to University of Babylon.

Author Contributions All authors contributed to the study's conception and design. Material preparation, data collection and analysis were performed by Ali Hussein Abdel-Amir and Majeed Ali Habeeb The first draft of the manuscript was written by Majeed Ali Habeeb and all authors commented on previous versions of the manuscript. All authors read and approved the final manuscript.

Funding No funding.

Data Availability No datasets were generated or analysed during the current study.

Declarations

Ethics Approval The research is not involving the studies on human or their data.

Consent to Participate Consent.

Consent for Publication Consent.

Competing Interests The authors declare no competing interests.

References

1. Singh R, Smitha MS, Singh SP (2014) The role of nanotechnology in combating multi-drug resistant bacteria. J Nanosci Nanotechnol 14(7):1–10. https://doi.org/10.1166/jnn.2014.9527
2. Hadi AH, Habeeb MA (2021) Effect of CdS nanoparticles on the optical properties of (PVA-PVP) blends. J Mech Eng Res Dev 44(3):265–274. https://www.jmerd.net/03-2021-265-274/
3. Al-Sharifi NK, Habeeb MA (2023) Synthesis and exploring structural and optical properties of ternary PS/SiC/Sb2O3 nanocomposites for optoelectronic and antimicrobial applications. Silicon. https://doi.org/10.1007/s12633-023-02418-2
4. Mohammed AA, Habeeb MA (2023) Modification and development of the structural, optical and antibacterial characteristics of PMMA/Si3N4/TaC nanostructures. Silicon. https://doi.org/10.1007/s12633-023-02426-2
5. Dwech MH, Habeeb MA, Mohammed AH (2022) Fabrication and evaluation of optical characterstic of (PVA-MnO2–ZrO2) nanocomposites for nanodevices in optics and photonics. Ukr J Phys 67(10):757–762. https://doi.org/10.15407/ujpe67.10.757
6. Tran TH, Nguyen VT (2014) Copper oxide nanomaterials prepared by solution methods, some properties, and potential applications: a brief review. Int Sch Res Not 2014:14
7. Yan Z, Hu Q, Jiang F, Lin S, Li R, Chen S (2023) Mechanism and technology evaluation of a novel alternating-arc-based directed energy deposition method through polarity-switching self-adaptive shunt. Addit Manuf 67:103504. https://doi.org/10.1016/j.addma.2023.103504
8. Habeeb MA, Mahdi WS (2019) Characterization of (CMC-PVP-Fe_2O_3) nanocomposites for gamma shielding application. Int J Emerg Trends Eng Res 7(9):247–255. https://doi.org/10.30534/ijeter/2019/06792019
9. Mahdi SM, Habeeb MA (2023) Tailoring the structural and optical features of (PEO–PVA)/(SrTiO3–CoO) polymeric nanocomposites for optical and biological applications. Polym Bull. https://doi.org/10.1007/s00289-023-04676-x
10. Habeeb MA, Jaber ZS (2022) Enhancement of structural and optical properties of CMC/PAA blend by addition of zirconium carbide nanoparticles for optics and photonics applications. East Eur J Phys 4:176–182. https://doi.org/10.26565/2312-4334-2022-4-18
11. Hashim A, Abbas MH, Al-Aaraji NAH, Hadi A (2023) Controlling the morphological, optical and dielectric characteristics of PS/SiC/CeO2 nanostructures for nanoelectronics and optics fields. J Inorg Organomet Polym Mater 33(1):1–9. https://doi.org/10.1007/s10904-022-02485-9
12. Hashim A, Habeeb MA (2018) Structural and optical properties of (biopolymer blend-metal oxide) bionanocomposites for humidity sensors. J Bionanosci 12(5):660–663. https://doi.org/10.1166/jbns.2018.1578
13. Gao S, Li H, Huang H, Kang R (2022) Grinding and lapping induced surface integrity of silicon wafers and its effect on chemical mechanical polishing. Appl Surf Sci 599:153982. https://doi.org/10.1016/j.apsusc.2022.153982
14. Habeeb MA, Kadhim WK (2014) Study the optical properties of (PVA-PVAC-Ti) nanocomposites. J Eng Appl Sci 9(4):109–113. https://doi.org/10.36478/jeasci.2014.109.113
15. Kuang W, Wang H, Li X, Zhang J, Zhou Q, Zhao Y (2018) Application of the thermodynamic extremal principle to diffusion-controlled phase transformations in Fe-C-X alloys:

modeling and applications. Acta Mater 159:16–30. https://doi.org/10.1016/j.actamat.2018.08.008
16. Habeeb MA (2011) Effect of rate of deposition on the optical parameters of GaAs films. Eur J Sci Res 57(3):478–484
17. Zhao X, Fan B, Qiao N, Soomro RA, Zhang R, Xu B (2024) Stabilized Ti3C2Tx-doped 3D vesicle polypyrrole coating for efficient protection toward copper in artificial seawater. Appl Surf Sci 642:158639. https://doi.org/10.1016/j.apsusc.2023.158639
18. Habeeb MA, Hashim A, Hayder N (2020) Structural and optical properties of novel (PS-Cr_2O_3/$ZnCoFe_2O_4$) nanocomposites for UV and microwave shielding. Egypt J Chem 63:697–708. https://doi.org/10.21608/ejchem.2019.12439.1774
19. Wu Y et al (2023) Metastable structures with composition fluctuation in cuprate superconducting films grown by transient liquid-phase assisted ultra-fast heteroepitaxy. Mater Today Nano 24:100429. https://doi.org/10.1016/j.mtnano.2023.100429
20. Lu Y et al (2017) Supporting information for : mixed-mode operation of hybrid phase-change nanophotonic circuits. Mixed-mode operation of hybrid phase-change nanophotonic circuits. Nano Letters 17(1):150–155. https://doi.org/10.1021/acs.nanolett.6b03688
21. Zhu Q, Chen J, Gou G, Chen H, Li P (2017) Ameliorated longitudinal critically refracted -attenuation velocity method for Welding residual stress measurement. J Mater Process Tech 246:267–275. https://doi.org/10.1016/j.jmatprotec.2017.03.022
22. Muhammad I, Ali A, Zhou L, Zhang W, Wong PKJ (2022) Vacancy-engineered half-metallicity and magnetic anisotropy in CrSI semiconductor monolayer. J Alloys Compd 909:164797. https://doi.org/10.1016/j.jallcom.2022.164797
23. AlSharifi NK, Habeeb MA (2023) Improvement structural and dielectric properties of PS/SiC/Sb2O3 nanostructures for nanoelectronicss devices. East Eur J Phys 2:341–347. https://doi.org/10.26565/2312-4334-2023-2-40
24. Huang Z, Luo P, Wu Q, Zheng H (2022) Constructing one-dimensional mesoporous carbon nanofibers loaded with NaTi2(PO4)3 nanodots as novel anodes for sodium energy storage. J Phys Chem Solids 161:110479. https://doi.org/10.1016/j.jpcs.2021.110479
25. Zhu ZY, Liu YL, Gou GQ, Gao W, Chen J (2021) Effect of heat input on interfacial characterization of the butter joint of hot-rolling CP-Ti/Q235 bimetallic sheets by laser + CMT. Sci Rep 11(1):1–11. https://doi.org/10.1038/s41598-021-89343-9
26. Phukan P, Saikia D (2013) Optical and structural investigation of CdSe quantum dots dispersed in PVA matrix and photovoltaic applications. Int J Photoenergy 2013:1–5
27. Fu ZH et al (2020) Hydrogen embrittlement behavior of SUS301L-MT stainless steel laser-arc hybrid welded joint localized zones. Corros Sci 164:108337. https://doi.org/10.1016/j.corsci.2019.108337
28. Habeeb MA, Hamza RSA (2018) Synthesis of (polymer blend –MgO) nanocomposites and studying electrical properties for piezoelectric application. Indonesian J Electr Eng Inf 6(4):428–435. https://doi.org/10.11591/ijeei.v6i1.511
29. Kadham Algidsawi AJ, Hashim A, Hadi A, Habeeb MA, Abed HH (2022) Influence of MnO2 nanoparticles addition on structural, optical and dielectric characteristics of PVA/PVP for pressure sensors. Phys Chem Solid State 23(2):353–360. https://doi.org/10.15330/pcss.23.2.353-360
30. An Z, Huang Y, Zhang R (2023) High-temperature multispectral stealth metastructure from the microwave-infrared compatible design. Compos Part B Eng 259:110737. https://doi.org/10.1016/j.compositesb.2023.110737
31. Hashim A, Habeeb MA, Jebur QM (2020) Structural, dielectric and optical properties for (polyvinyl alcohol-polyethylene oxide manganese oxide) nanocomposites. Egypt J Chem 63:735–749. https://doi.org/10.21608/ejchem.2019.14849.1901
32. Jiang C et al (2022) Spin-orbit-engineered selective transport of photons in plasmonic nanocircuits with panda-patterned transporters. ACS Photonics 1–5. https://doi.org/10.1021/acsphotonics.2c00841
33. Zhang Y et al (2023) Enhanced energy storage performance of polyethersulfone-based dielectric composite via regulating heat treatment and filling phase. J Alloys Compd 960:170539. https://doi.org/10.1016/j.jallcom.2023.170539
34. Hashim A, Kadham Algidsawi AJ, Ahmed H, Hadi A, Habeeb MA (2021) Synthesis of PVA/PVP/SnO_2 nanocomposites: structural, optical, and dielectric characteristics for pressure sensors. Nanosistemi Nanomateriali Nanotehnologii 19(2):353–362. https://doi.org/10.15407/nnn.19.02.353
35. Zhang X, Tang Y, Zhang F, Lee CS (2016) A novel aluminum-graphite dual-ion battery. Adv Energy Mater 6(11):1–7. https://doi.org/10.1002/aenm.201502588
36. Wang H, Huang Z, Zeng X, Li J, Zhang Y, Hu Q (2023) Enhanced anticarbonization and electrical performance of epoxy resin via densified spherical boron nitride networks. ACS Appl Electron Mater 5(7):3726–3732. https://doi.org/10.1021/acsaelm.3c00451
37. Hashim A, Kadham AJ, Hadi A, Habeeb MA (2021) Determination of optical parameters of polymer blend/nanoceramics for electronics applications. Nanosistemi Nanomateriali Nanotehnologii 19(2):327–336. https://doi.org/10.15407/nnn.19.02.327
38. Habeeb MA (2014) Dielectric and optical properties of (PVAc-PEG-Ber) biocomposites. J Eng Appl Sci 9(4):102–108. https://doi.org/10.36478/jeasci.2014.102.108
39. Hu G, Ying S, Qi H, Yu L, Li G (2023) Design, analysis and optimization of a hybrid fluid flow magnetorheological damper based on multiphysics coupling model. Mech Syst Signal Process 205:110877. https://doi.org/10.1016/j.ymssp.2023.110877
40. Dalven R, Gill R (1967) Electrical properties of β-Ag2Te and β-Ag2Se from 4.2° to 300° K. J Appl Phys 38(2):753–756
41. Mahdi SM, Habeeb MA (2022) Synthesis and augmented optical characteristics of PEO–PVA–SrTiO3–NiO hybrid nanocomposites for optoelectronics and antibacterial applications. Opt Quant Electron 54:854. https://doi.org/10.1007/s11082-022-04267-6
42. Li Y, Porwal H, Huang Z, Zhang H, Bilotti E, Peijs T (2016) Enhanced thermal and electrical properties of polystyrene-graphene nanofibers via electrospinning. J Nanomater 2016:1–6
43. Habeeb MA, Abdul Hamza RS (2018) Novel of (biopolymer blend-MgO) nanocomposites: fabrication and characterization for humidity sensors. J Bionanosci 12:328–335. https://doi.org/10.1166/jbns.2018.1535
44. Du S et al (2022) Auger scattering dynamic of photo-excited hot carriers in nano-graphite film. Appl Phys Lett 121(18):181104. https://doi.org/10.1063/5.0116720
45. Mathew CM, Kesavan K, Rajendran S (2015) Structural and electrochemical analysis of PMMA based gel electrolyte membranes. Int J Electrochem 2015:1–7
46. Habeeb MA, Jaber ZS, Radi WH (2023) Synthesis and characterization of (PVA-CoO-ZrO2) nanostructures for nanooptoelectronic fields. East Eur J Phys 2:228–233. https://doi.org/10.26565/2312-4334-2023-2-25
47. Rajesh K, Crasta V, Rithin Kumar N, Shetty G, Rekha P (2019) Structural, optical, mechanical and dielectric properties of titanium dioxide doped PVA/PVP nanocomposite. J Polym Res 26(4):1–10
48. Mahdi SM, Habeeb MA (2022) Evaluation of the influence of SrTiO3 and CoO nanofillers on the structural and electrical polymer blend characteristics for electronic devices. Digest J Nanomater Biostruct 17(3):941–948. https://doi.org/10.15251/DJNB.2022.173.941
49. Habeeb MA, Mohammed AH (2023) Fabrication and tailored optical and electrical characteristics of Co2O3/SiC nanostructures doped PVA for multifunctional technological

applications. Opt Quant Electron 55:791. https://doi.org/10.1007/s11082-023-05061-8
50. Algidsawi AJK, Hashim A, Hadi A, Habeeb MA (2021) Exploring the characteristics of SnO_2 nanoparticles doped organic blend for low cost nanoelectronics applications. Semicond Phys Quantum Electron Optoelectron 24(4):472–477. https://doi.org/10.15407/spqeo24.04.472
51. Wang J-C, Karmakar RS, Lu Y-J, Huang C-Y, Wei K-C (2015) Characterization of piezoresistive PEDOT: PSS pressure sensors with inter-digitated and cross-point electrode structures. Sensors 15(1):818–831
52. Mahdi SM, Habeeb MA (2023) Low-cost piezoelectric sensors and gamma ray attenuation fabricated from novel polymeric nanocomposites. AIMS Mater Sci 10(2):288–300. https://doi.org/10.3934/matersci.2023015
53. Mohammed AA, Habeeb MA (2023) Effect of Si_3N_4/TaC nanomaterials on the structural and electrical characteristics of poly methyl methacrylate for electrical and electronics applications. East Eur J Phys 2:157–164. https://doi.org/10.26565/2312-4334-2023-2-15
54. Habeeb MA, Hashim A, Hayder N (2020) Fabrication of (PS-Cr_2O_3/$ZnCoFe_2O_4$) nanocomposites and studying their dielectric and fluorescence properties for IR sensors. Egypt J Chem 63:709–717. https://doi.org/10.21608/ejchem.2019.13333.1832
55. Jebur QM, Hashim A, Habeeb MA (2020) Structural, A.C electrical and optical properties of (polyvinyl alcohol-polyethylene oxide-aluminum oxide) nanocomposites for piezoelectric devices. Egypt J Chem 63:719–734. https://doi.org/10.21608/ejchem.2019.14847.1900
56. Habeeb MA, Rahdi WH (2023) Titanium carbide nanoparticles filled PVAPAAm nanocomposites, structural and electrical characteristics for application in energy storage. Opt Quant Electron 55:334. https://doi.org/10.1007/s11082-023-04639-6
57. Mahdi SM, Habeeb MA (2022) Fabrication and tailored structural and dielectric characteristics of (SrTiO3/ NiO) nanostructure doped (PEO/PVA) polymeric blend for electronics fields. Phys Chem Solid State 23(4):785–792. https://doi.org/10.15330/pcss.23.4.785-792
58. Hadi AH (2021) Habeeb MA The dielectric properties of (PVA-PVP-CdS) nanocomposites for gamma shielding applications. J Phys: Conf Ser 1973(1):012063. https://doi.org/10.1088/1742-6596/1973/1/012063
59. Hayder N, Habeeb MA, Hashim A (2020) Structural, optical and dielectric properties of (PS-In_2O_3/$ZnCoFe_2O_4$) nanocomposites. Egypt J Chem 63:577–592. https://doi.org/10.21608/ejchem.2019.14646.1887